

The massive white dwarf in the recurrent nova T CrB

T. Shahbaz,¹ M. Somers,² B. Yudin,³ and T. Naylor²

¹*Department of Astrophysics, Nuclear Physics Building, Keble Road, Oxford, OX1 3RH, UK*

²*Department of Physics, Keele University, Keele, Staffordshire, ST5 5BG, UK*

³*Sternberg Astronomical Institute, University of Moscow, Russia*

14 October 2018

ABSTRACT

We have obtained *I*, *J*, *H* and *K* band light curves of the recurrent nova T CrB. We find that we can only fit the *J* band light curve with a Roche-lobe filling secondary star and a dark spot of radius 11° – 26° (90 per cent confidence) centred at the inner Lagrangian point. We obtain limits to the binary inclination of 38° – 46° (90 per cent confidence) which when combined with the value for the mass function allows us to determine the mass of the compact object to be 1.3 – $2.5 M_\odot$ (90 per cent confidence). This mass range is consistent with the Chandrasekhar limiting white dwarf mass, and so we provide evidence needed to support the outbursts in recurrent novae in terms of a thermonuclear runaway process on the surface of a massive $\sim 1.4 M_\odot$ white dwarf.

Key words: stars: fundamental parameters – novae, cataclysmic variables – stars: individual: T CrB.

1 INTRODUCTION

T CrB is a well studied recurrent nova with an M giant component. It underwent nova like outbursts in 1866 and 1946, with light curves which were very similar. They are characterised by having a fast rise to maximum and by a secondary, fainter maximum occurring $\simeq 100$ days later. The secondary maximum has a very slow decay time (> 10 years).

Two competing models have been suggested to account for the peculiar outburst behaviour. One suggestion is that the outburst is due to a thermonuclear runaway (TNR) on the surface of a white dwarf primary. If this is the case then the short recurrence time implies that the white dwarf must have a mass very close to the Chandrasekhar limit ($1.4 M_\odot$; Chandrasekhar 1939) and that the ejected envelope should be relatively small (Webbink 1976a). Alternatively Plavec, Ulrich & Polidan (1973) and Webbink (1976a) proposed that the hot component is a normal main sequence star, with eruptions being caused by sudden mass accretion events. This model can nicely account for a fading of the system before the outburst and the double maximum in the outburst light curve, however one is confined to a main sequence accretor. Selvelli, Cassatella & Gilmozzi (1992) have found evidence from IUE spectra that the accretor is a white dwarf. They point to three pieces of evidence: (1) the bulk of the luminosity is emitted in the UV with little contribution from the hot component in the optical, (2) strong He II and N V emission lines suggest temperatures of $\simeq 10^5 K$ and (3) the observed large rotational broadening of the high excitation lines.

Table 1. Log of observations

Band	Date of observation	Number of points
I	Sep 1994 – Jun 1995	420 points
J	Aug 1987 – Jun 1995	102 points
H	Sep 1987 – Mar 1990	12 points
K	Sep 1988 – Jun 1995	58 points

Sandford (1949) first detected radial velocity variations in the emission lines while Kraft (1958) established a spectroscopic period of the system to be 227.6 days. Kraft (1958) also derived a mass ratio ($q = M_1/M_2$) of 0.71 (where M_1 is the giant component) based in part on radial velocities extracted from emission lines originating in material accreting onto the primary. We now view radial velocities derived from such emission lines as unsound and thus reject his value for q . Kenyon & Garcia (1986) obtained a lower limit to the binary mass ratio of 2.5 by determining an upper limit to the rotational broadening of the giant star.

In this paper we present a photometric study of the ellipsoidal variations of the M giant. By fitting the *J* band light curve we determine the binary inclination and hence determine the mass of the compact component.

2 PHOTOMETRIC OBSERVATIONS

The infrared observations were taken at the Crimean Astrophysical Observatory of Sternberg Astronomical Institute using an InSb photometer on the 1.25m telescope. We obtained J (12500Å), H (16500Å) and K (22000Å) band photometry of T CrB during the period 1987–1995 (see Table 1). Most of the data have an accuracy of better than 0.02 mags. The standard BS 5947 was used as a comparison star and BS 5972 as a check star.

The I (8500Å) band data were taken through a Johnson filter with the 0.6m Thornton Reflector at Keele Observatory during 1994–1995 using a Santa Barbara Instruments ST-6 CCD camera mounted at the f/4.5 Newtonian focus. The dark current was subtracted for each image using a median stack of several dark frames. Relative photometry was carried out using the routine described in Shahbaz, Naylor & Charles (1994).

The individual data for each band were then folded on the ephemeris given by Kenyon & Garcia (1986) and then binned in orbital phase (see Fig. 1).

3 THE M GIANT ELLIPSOIDAL VARIATIONS

The observed ellipsoidal variations are primarily due to the giant star presenting differing aspects of its distortion as it orbits the compact object. By measuring the amplitude of this modulation, the binary inclination can be determined (see Shahbaz, Naylor & Charles 1993 and references within). The J band data covers ~ 11 orbital cycles and the individual points fit the same light curve. This suggests that the M giant does not vary its intrinsic brightness by more than a few hundredths of a magnitude (Yudin & Munari 1993). The erratic and quasi-periodic variations, with amplitudes larger than the ellipsoidal modulation of the M giant, make interpreting the optical light curves very difficult (Webbink 1976b; Lines et al. 1988; Peel 1990). These effects reduce at longer wavelengths, and they should be absent in the infrared, where the emission from the M giant star dominates. The amplitude of our I band light curve is ~ 0.35 mags, which is more than a factor 2 greater than that expected for the ellipsoidal variations of the M giant inclined at 40° (see section 4). In light of the quasi-periodic behaviour of the optical light curves, we only fit the J band light curve, where one expects these uncertainties to be reduced.

4 THE CLASSICAL MODEL

In the M star of a cataclysmic variable secondary, the envelope is deeply convective. Sarna (1989) obtained the gravity-darkening using a modified form of Lucy's (Lucy 1967) gravity-darkening law appropriate for a star with a convective envelope. One can model the ellipsoidal variations as a function of the binary mass ratio q , inclination i , the effective temperature of the secondary star T_{eff} , the limb-darkening coefficient and gravity-darkening exponent β .

Using the ellipsoidal model described in Shahbaz, Naylor & Charles (1993) we performed a least-squares fit to the J band light curves, grid searching the variables q and i . We used $T_{\text{eff}}=3500$ K, $\beta=0.08$ and i in the range 20° – 90° . From optical spectroscopy, Kenyon & Garcia (1986) estimate that

the mass ratio must be at least 2.5. We therefore search q in the range 2.0–10.0. The appropriate limb-darkening coefficient for each wavelength and temperature was extrapolated using the values given by Al-Naimiy (1978). We obtained a minimum χ^2 of $\chi^2_{\nu}=2.9$ at $q=3$, $i=48^\circ$. As one can see, this fit (dotted line in Fig. 2) does not describe the data well.

In an attempt to explain the large difference between the minima we explored fits using different values for the gravity darkening exponent. We computed fits by grid searching the variables q , i and β . As explained in the Appendix, we find that the blackbody assumption for the H and K band data is poor. Therefore, in what follows we only use the J band data where the blackbody assumption is more robust. Fig. 3 shows the χ^2 fit in the $\beta-i$ plane, obtained by collapsing the minimum χ^2 solutions along the q axis onto the $\beta-i$ plane. In effect we have let q run as a free parameter. We obtained a minimum χ^2 of 2.5 at $q=3$, $i=43^\circ$ and $\beta=0.20$. The limits derived are $i=35$ – 51° and $\beta=0.05$ – 0.36 (68 per cent confidence). The 68 and 90 per cent confidence regions (solid and dashed lines respectively) are shown, calculated according to Lampton, Margon & Bowyer (1976) for 2 parameters, after the error bars had been scaled to give a minimum χ^2_{ν} of 1. The solid line in Fig. 2 shows the best fit to the J band light curve. As one can see the fit to the data points near phase 0.5 is not very good. There still is an extra component which is introducing an uncertainty of about 60 per cent to the light curves. In the next section we try to explain the large difference between the minima in the J band light curves in terms of a dark spot located at the inner Lagrangian point.

5 THE NEED FOR A DARK SPOT

Star-spots have been observed in other interacting binary stars, in particular in those systems in which the mass-losing component is a late-type star, e.g. RS CVn systems (Rodono 1983). Also there is much stellar activity associated with M stars. Peel (1990) presents marginal evidence for stellar activity in T CrB near phase 0.5 from the observations of ultraviolet flares (Ianna 1964) and the visual brightening of T CrB.

In an attempt to explain the large difference between the minima of the J band light curve, we fit the light curve with the ellipsoidal modulation of the secondary star plus a dark spot. Since the maxima in the light curve are almost equal, for simplicity we centred the spot around the inner Lagrangian point (L_1). The spot is described as a circle extending to a latitude R_{spot}° away from the L_1 point. The effective temperature in the dark spot region is lower than it would have been in the absence of the spot by 750 K. This is the typical observed temperature difference in RS CVn systems and T Tauri stars (Rodono 1986).

Using the nominal value for the gravity darkening exponent for a convective star (0.08), we obtained fits in the q , i and R_{spot} plane. We find $\chi^2_{\nu,\text{min}} = 2.6$ at $i=40^\circ$ and $R_{\text{spot}}=20^\circ$. The 90 per cent confidence limits are $i=38$ – 46° and $R_{\text{spot}}=11$ – 26° (see Fig. 4). Lowering the spot temperature by a further 250 K changes the inclination by $< 1^\circ$. The dashed line in Fig. 2 shows the best fits to the J band light curve using a dark spot of size 20° . As one can see the fit to the light curve has improved.

That using large values for β gives fits of similar quality to that using a dark spot placed around the L_1 point is not surprising. If we look at the temperature distribution across the secondary star for $\beta=0.08$ and 0.20 (see Fig. 5), then one can see that the effect of high values for β is to simulate two regions of low temperature around the inner Lagrangian point and the opposite hemisphere of the secondary star. This effect can to some degree be reproduced by adding a dark spot round the L_1 point.

6 THE EVOLUTIONARY STATUS OF THE SECONDARY

In this section we use theoretical equations which describe the luminosity and radius of the giant star in order to determine the predicted mass transfer rate. For evolved secondary stars, i.e. stars on the first red giant branch and asymptotic giant-branch stars Joss, Rappaport & Lewis (1987) give the results of fitting the luminosity (L) and radius (R) core mass (M_c) relations to numerical models, for $0.17 M_\odot \lesssim M_c \lesssim 1.4 M_\odot$. They give the parameterisations

$$\frac{L_2}{L_\odot} = \frac{10^{5.3} M_c^6}{1 + 10^{0.4} M_c^4 + 10^{0.5} M_c^5} \quad (1)$$

$$\frac{R_2}{R_\odot} = \frac{3.7 \times 10^3 M_c^6}{1 + M_c^3 + 1.75 M_c^4}. \quad (2)$$

As noted by King (1988), there is little radius expansion for $M_c \gtrsim 0.7$ and so the mass transfer rates will be very low. However, for $M_c \lesssim 0.7$ the denominators in the above equations are ~ 1 . So if mass transfer is to occur, the stellar radius R_2 must equal the Roche-lobe radius given by Paczynski's formula Paczynski (1971)

$$\frac{R_L}{a} = 0.462 \left(\frac{M_2}{M_1 + M_2} \right)^{1/3}. \quad (3)$$

Eliminating the binary separation a by use of Kepler's law with the binary period of 227.53 days, the requirement $R_2=R_L$ implies

$$0.0011 = M_c^6 M_2^{-0.5}. \quad (4)$$

The limiting cases for M_c are given by the extreme values of M_2 . We must have $M_2 \geq M_c$, while the secondary would have not left the main sequence if M_c/M_2 were less than the Schönberg-Chandrasekhar limiting value of 0.17, implying $M_2 \leq 5.88 M_c$.

Following King (1993) we find the following values for the two limiting cases (see Table 2). The limiting cases give M_c , which when used in equations (1) and (2) give L_2 and R_2 . Using Stefan's Law then gives T_{eff} . King (1988) gives the mass transfer rate as a function of M_c and M_2

$$-\dot{M}_2 = 6.4 \times 10^{-6} M_2 M_c^5 \text{ } M_\odot \text{ yr}^{-1} \quad (5)$$

which can also be used to obtain the predicted mass transfer rates for the two limiting cases. The lower limit to the compact object mass can also be determined by using the value of the mass function and assuming maximum inclination and the two limiting values for M_2 . The maximum and minimum solutions correspond to T CrB being near the beginning and end of its evolution respectively. One can see that the observed spectral type for the secondary star, M3

III ($T_{\text{eff}} = 3500$ K) and the observed average mass accretion rate of $2.3 \times 10^{-8} M_\odot \text{ yr}^{-1}$ (Selvelli et al. 1992) lie in between the predicted solutions.

7 DISCUSSION

7.1 The mass of the white dwarf

Here we determine limits to the mass of the compact object using the limits derived for the binary inclination by fitting the J band light curve. Using the equation for the mass function ($f(M)=0.30 \pm 0.01 M_\odot$; Kenyon & Garcia 1986), with values for i and M_2 , we can determine M_1 . Fig. 6 shows the M_1 , M_2 solutions at the 68 and 90 per cent confidence levels. We also show the limits placed on the mass ratio of > 2.5 and the evolutionary constraints on the mass of the secondary star (see section 6). It can be seen that the mass of the compact object is forced to lie in the range 1.3–2.5 M_\odot (90 per cent confidence).

Ramsayer et al.(1993) and Harrison, Johnson & Spyromilio (1993) show low resolution K band spectra of T CrB. They find that the spectra resemble that of a late type giant star, and comparison with M giants from Kelmann & Hall (1986) suggests a spectral type of M2–M5 III. Fig. 7 shows the flux distribution of T CrB. The optical and infrared magnitudes were taken from Munari (1992) and were dereddened using $E_{B-V}=0.15$ (Selvelli, Cassatella & Gilmozzi 1992). As one see the flux distribution of T CrB can be well described by a M3 III Kurucz model atmosphere spectrum (Kurucz 1992). Both the infrared spectra and the flux distribution of T CrB suggest that there is little contamination of the IR flux. A 10 per cent contamination of the J band flux would increase the binary inclination by $\sim 3^\circ$, which would decrease the mass of the compact object by only $\sim 0.3 M_\odot$.

7.2 The nature of the white dwarf

The main ingredients of the thermonuclear runaway (TNR) models proposed to explain the outburst behaviour in recurrent novae are

- The luminosity at maximum light needs to be greater than the Eddington luminosity,
- the mass accretion rates during quiescence must be high, and
- the white dwarf must be very massive ($\sim 1.4 M_\odot$).

Selvelli, Castella & Gilmozzi (1992) have shown that the outburst in T CrB was indeed super Eddington and that the mass accretion rate during quiescence is very high ($2.3 \times 10^{-8} M_\odot \text{ yr}^{-1}$). In the TNR model the white dwarf mass needs to be close to the Chandrasekhar maximum mass for a white dwarf of 1.4 M_\odot , or else it cannot accrete enough material from the red giant companion in a short enough time to produce the short recurrence time.

We have obtained limits to the mass of the compact object to be 1.3–2.5 M_\odot , which is consistent with the Chandrasekhar maximum mass for a white dwarf of 1.4 M_\odot (Chandrasekhar 1939). In Fig. 8 we show for comparison the mass distribution of white dwarfs, taken from Ritter & Kolb (1995). The compact object cannot be a neutron star because of the observed nova explosions; in neutron stars

Table 2. Extreme Evolutionary solutions for T CrB

Parameter	Minimum mass	Maximum mass
Secondary core mass M_c (M_\odot)	0.2894	0.3401
Secondary total mass M_2 (M_\odot)	0.2894	2.000
Secondary radius R_2 (R_\odot)	26.0	49.44
Secondary luminosity L_2 (L_\odot)	117.2	308.2
Secondary effective temperature T_{eff} (K)	3731	3445
Mass transfer rate $M_\odot \text{yr}^{-1}$	3.8×10^{-9}	5.8×10^{-8}
Primary mass M_1 (M_\odot)	> 0.64	> 1.56

the strong gravitational potential prevents material being ejected. Our mass estimates for the compact object are such that we can support a massive $1.4 M_\odot$ white dwarf thus providing support for the presently untested predictions of TNR theory; namely that recurrent novae occur on massive white dwarfs. White dwarfs with masses $> 1.2 M_\odot$ and mass accretion rates $> 10^{-8} M_\odot \text{yr}^{-1}$ are expected to be net accretors (Livio & Turan 1992). Since white dwarfs are not generally born with masses of $1.4 M_\odot$, our mass determination implies that the white dwarf is a net accretor; eventually it will exceed the Chandrasekhar critical mass and become a type Ia supernova.

8 CONCLUSIONS

We have tried to fit the observed J band light curve of T CrB with the classical Roche-lobe filling secondary star model with a gravity darkening exponent of 0.08. However, in order to explain the large difference between the minima in the J band light curve, we find that we can only fit the light curve with the addition of a dark spot centred at the inner Lagrangian point. We obtain the 90 per cent confidence limits to the binary inclination of 38° – 46° , which when combined with the mass function gives the mass range for the compact object to be 1.3 – $2.5 M_\odot$ (90 per cent confidence). This mass range is consistent with Chandrasekhar limiting white dwarf mass $\sim 1.4 M_\odot$.

ACKNOWLEDGEMENTS

We are grateful to those who support Keele Observatory, especially the local amateur astronomers who help maintain the telescopes, and ICL who have provided computing facilities. TS was supported by a PPARC postdoctoral fellowship, and TN by a PPARC Advanced fellowship. BY was supported by RFFI grants 96-02-16353 and 96-02-16794. The data analysis was carried out on the Keele and Oxford Starlink nodes using the ARK software.

REFERENCES

Al-Naimiy H.M., 1978, *Ap&SS*, 53, 181
Allard F., Hauschildt P.H., 1995, *ApJ*, 445, 433
Bailey J., 1975, *JBAA*, 85, 217
Chandrasekhar S., 1939, *An Introduction to the Study of Stellar Structure*, Chicago: University of Chicago Press
Harrison T.E., Johnson J.J., Spyromilio J., 1993, *AJ*, 105, 320
Ianna P.A., 1964, *ApJ*, 139, 780
Johnson H.L., 1966, *ARA&A*, 4, 193

Joss P.C., Rappaport S., Lewis W., 1987, *ApJ*, 319, 180
Kenyon S.J., Garcia M.R., 1986, *AJ*, 91, 125
King A.R., 1988, *QJRAS*, 29, 1
King A.R., 1993, *MNRAS*, 260, L5
Kraft R.P., 1958, *ApJ*, 127, 625
Kurucz R.L., 1992, *Rev., Mex. Astr. Astroph.*, 23, 45
Lines H.C., Lines R.D., McFaul T.G., 1988, *AJ*, 95, 1505
Lampton M., Margon B., Bowyer S., 1976, *ApJ*, 208, 177
Livio M., Truran J.W., 1992, *ApJ*, 695, 703
Lucy L.B., 1967, *ZfAp*, 65, 89
Munari U., Yudin B.F., Taranova O.G., Massone F., Marang F., Roberts H., Winkler H., Whitelock P.A., 1992, *A&ASS*, 93, 383
Peel M., 1990, *JBAA*, 100, 136
Paczynski B., 1971 *ARA&A*, 9, 183
Plavec M., Ulrich R.K., Polidan R.S., 1973, *PASP*, 85, 769
Ramseyer T.F., Dinerstein H.L., Lester D.F., Provencional J., 1993, *ApJ*, 106, 1191
Ritter H., Kolb U., 1995, in *X-ray Binaries*, eds, Lewin W H.G., van Paradijs J., and van den Heuvel E.P.J., CUP, p 578
Rodono R., 1983, *Adv. Space Res.* 1, No. 9, 225
Rodono R., 1986, in *Zeilik M., Gibson D.M., eds, Cool Stars, Stellar Systems and the Sun*, Springer-Verlag, Berlin, p. 475
Sarna M.J., 1989, *A&A*, 224, 98
Selvelli P.L., Castella A., Gilmozzi R., 1992, *ApJ*, 393, 289
Shahbaz T., Naylor T., Charles P.A., 1993, *MNRAS*, 265, 655
Shahbaz T., Naylor T., Charles P.A., 1994, *MNRAS*, 268, 756
Webbink R.F., 1976a, *Nat.*, 262, 271
Webbink R.F., 1976b, *AAVSO*, 5, 26
Yudin B., Munari U., 1993, *A&A*, 270, 165
Von Zeipel H., 1924, *MNRAS*, 84, 665

APPENDIX

In our model for the ellipsoidal variations of T CrB, we have assumed that each element on the surface of the secondary star emits blackbody radiation of a given temperature. The temperature of each element is governed by the gravity darkening law that is adopted, depending on the structure of the envelope of the secondary star. A real M giant will obviously not emit as a blackbody, but have rather a complex spectrum with many late type absorption features. The flux emanating per unit surface area of such an atmosphere may be significantly different to that from the same temperature blackbody. We can estimate the accuracy of the blackbody assumption for observations taken through different passbands by comparing the ratio of the blackbody fluxes to the model atmosphere fluxes for different temperatures.

The amplitude of an ellipsoidal light curve can to some degree be approximated by determining the ratio of flux emitted at two different temperatures, governed by the mean temperature of the secondary star at phase 0.0 and 0.5.

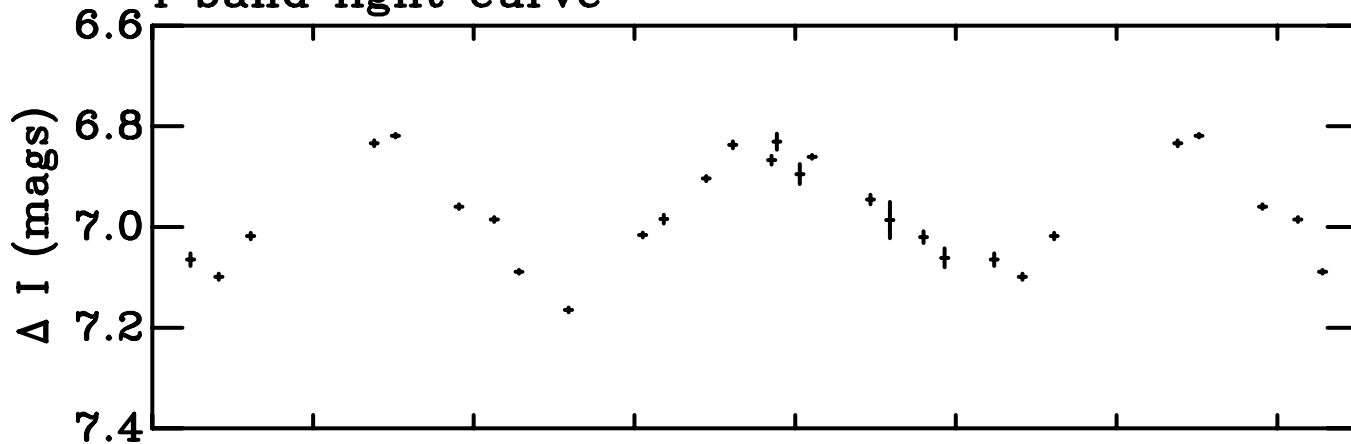
Table 3. Comparison of blackbody and model atmospheres fluxes

	Blackbody (mags)	Model atmospheres (mags)
$J_{3100K}-J_{3500K}$	0.48	0.46
$H_{3100K}-H_{3500K}$	0.38	0.47
$K_{3100K}-K_{3500K}$	0.31	0.54

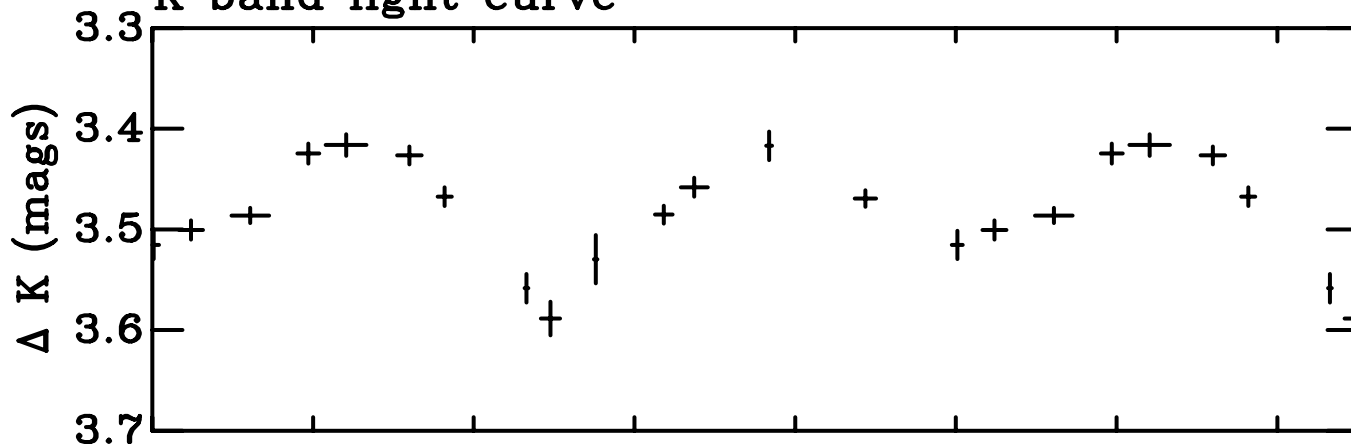
In order to estimate this temperature change we computed the ellipsoidal models with no surface temperature variation ($\beta=0.0$) and the maximum expected variation ($\beta=0.25$; see von Zeipel 1924). We then calculate the mean temperature difference between the gravity darkened inner face of the secondary and the unaltered uniform inner face of the secondary and find that the inner face of the secondary is on average cooler than the rest of the star by about 400 K.

We estimate the accuracy of the blackbody assumption by determining the magnitude difference between blackbody spectra at 3500 and 3100 K (after they have been folded through the response of the *J*, *H* and *K* filters) and comparing these values with those obtained using model atmospheres. The model atmosphere spectra for $\log g = 4.0$ were taken from Allard & Hauschildt (1995). We find the departure from the blackbody assumption in the *J*, *H* and *K* bands to be about 2, 9, and 24 per cent respectively.

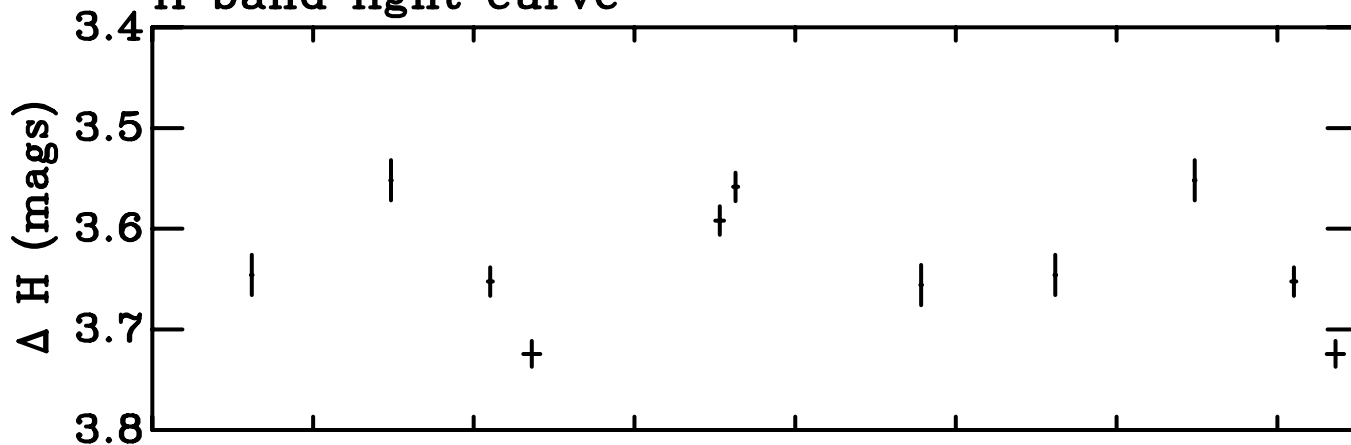
I band light curve



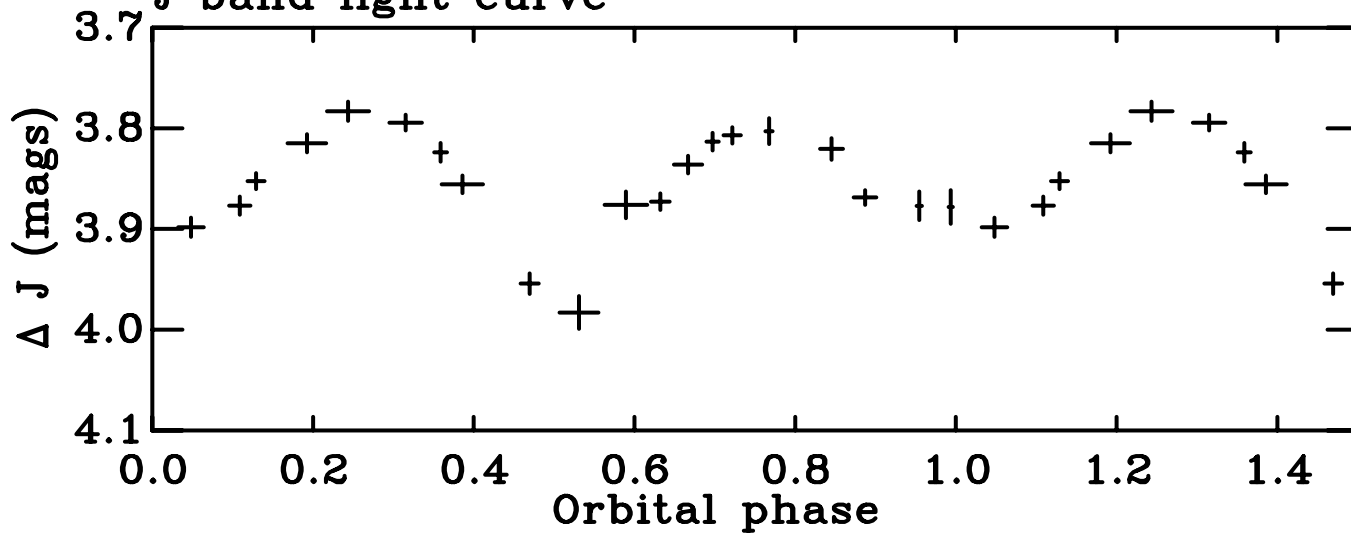
K band light curve

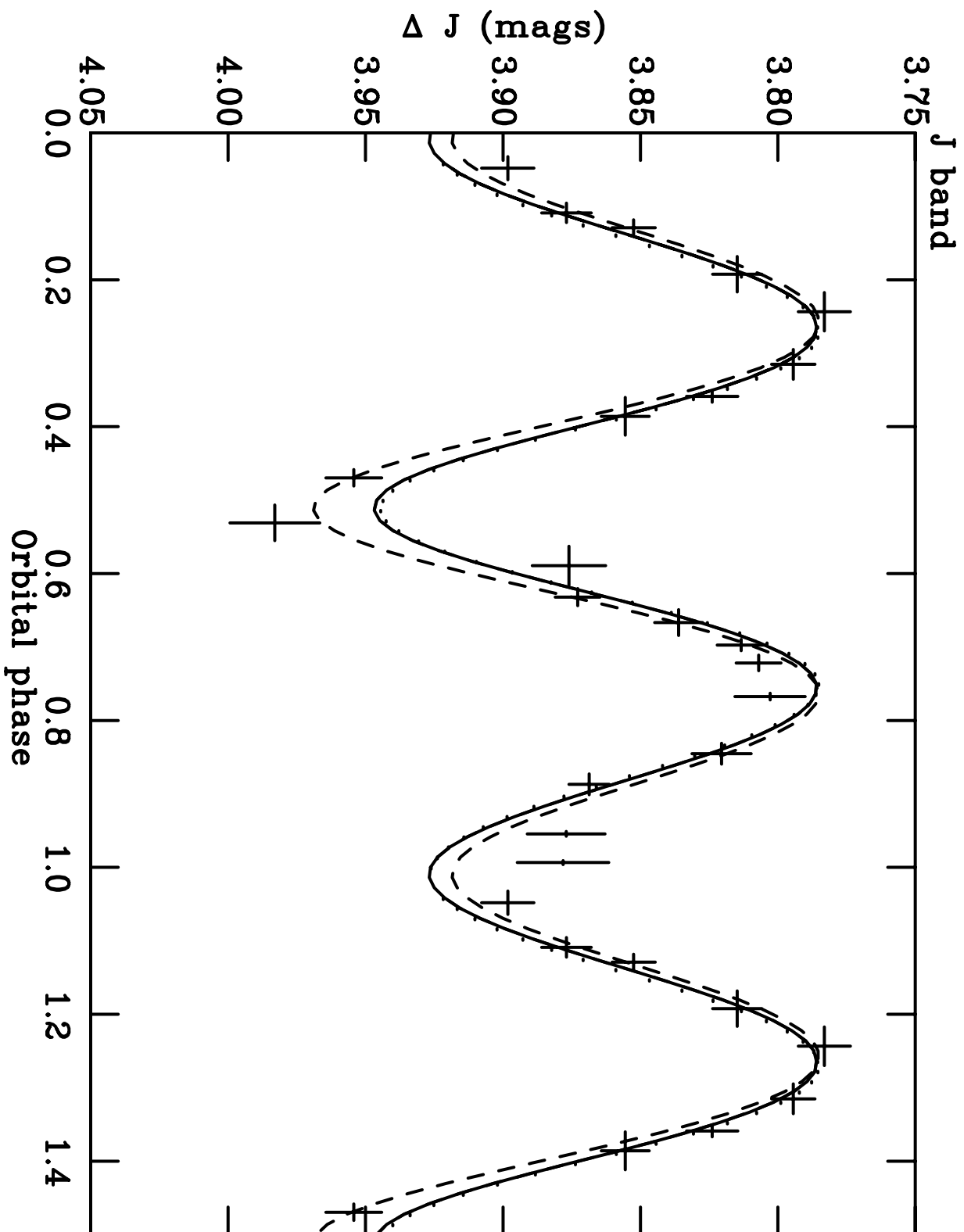


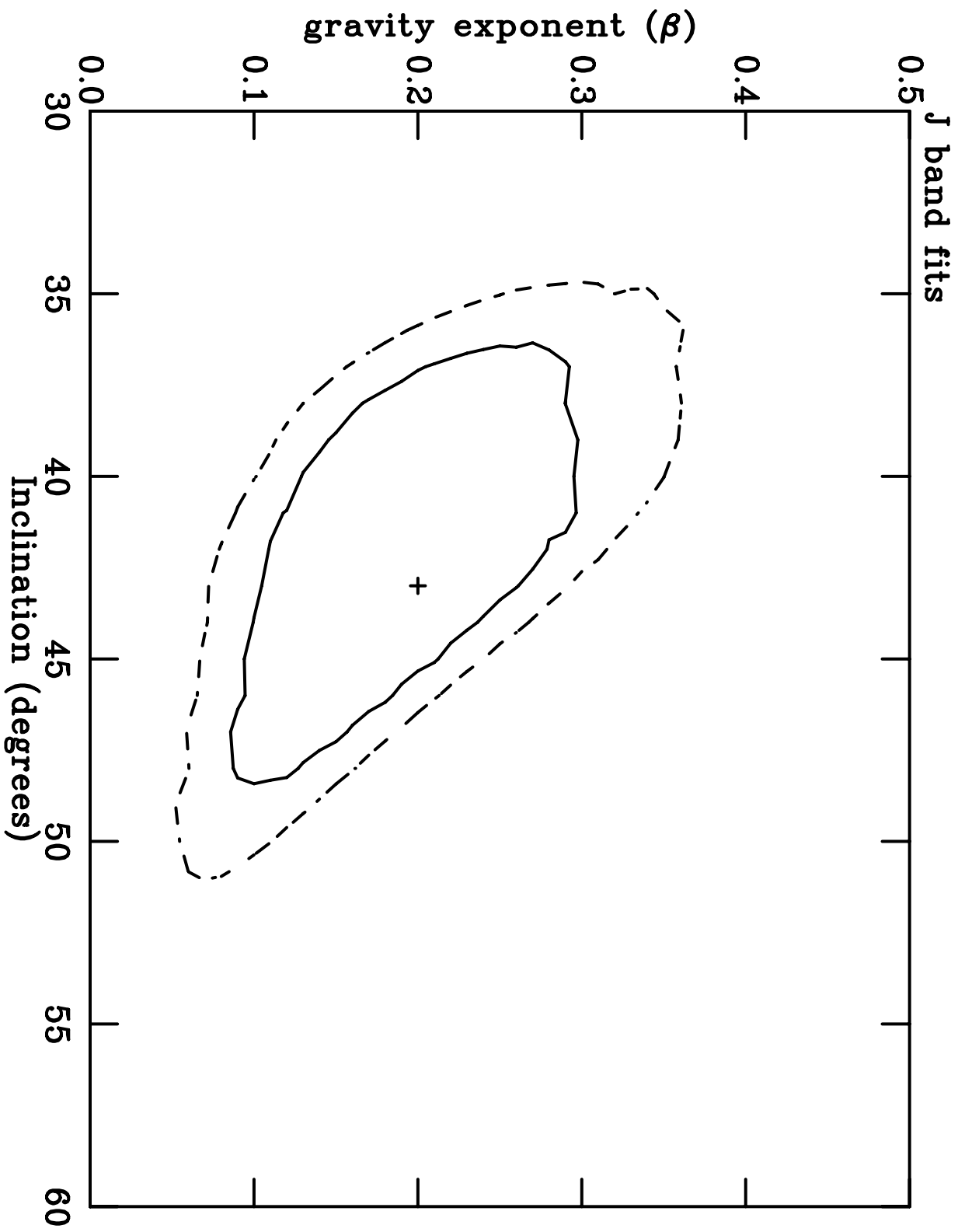
H band light curve

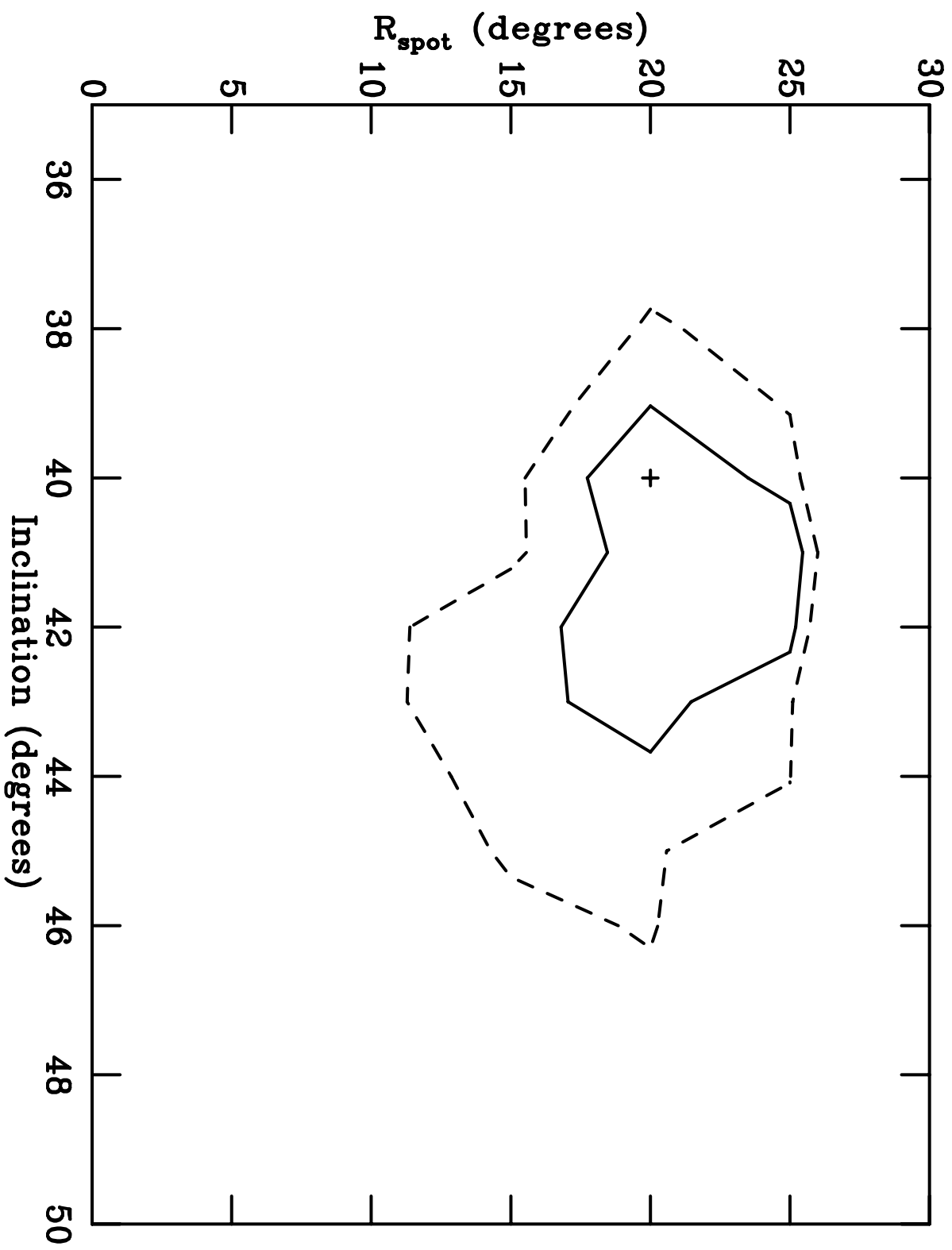


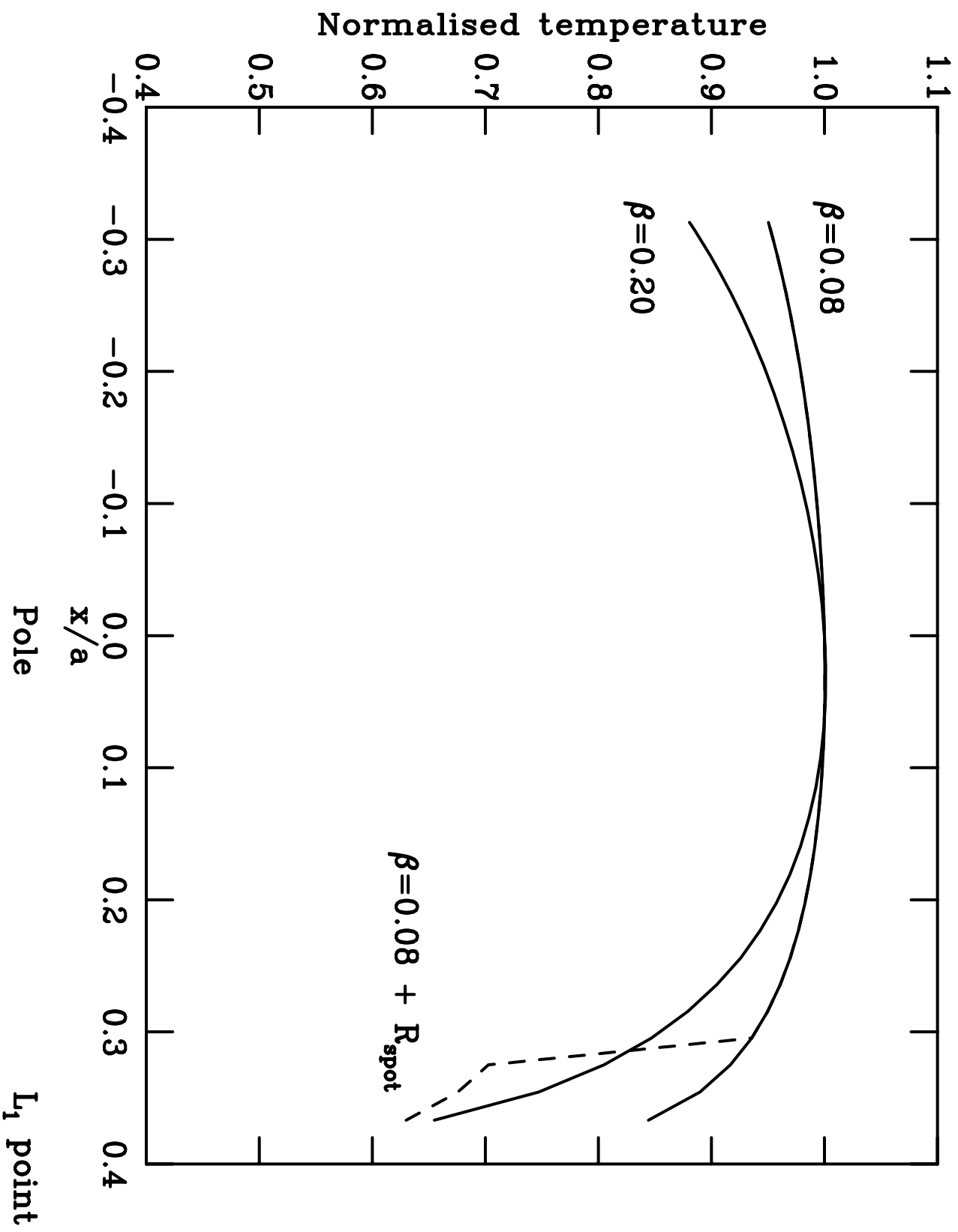
J band light curve

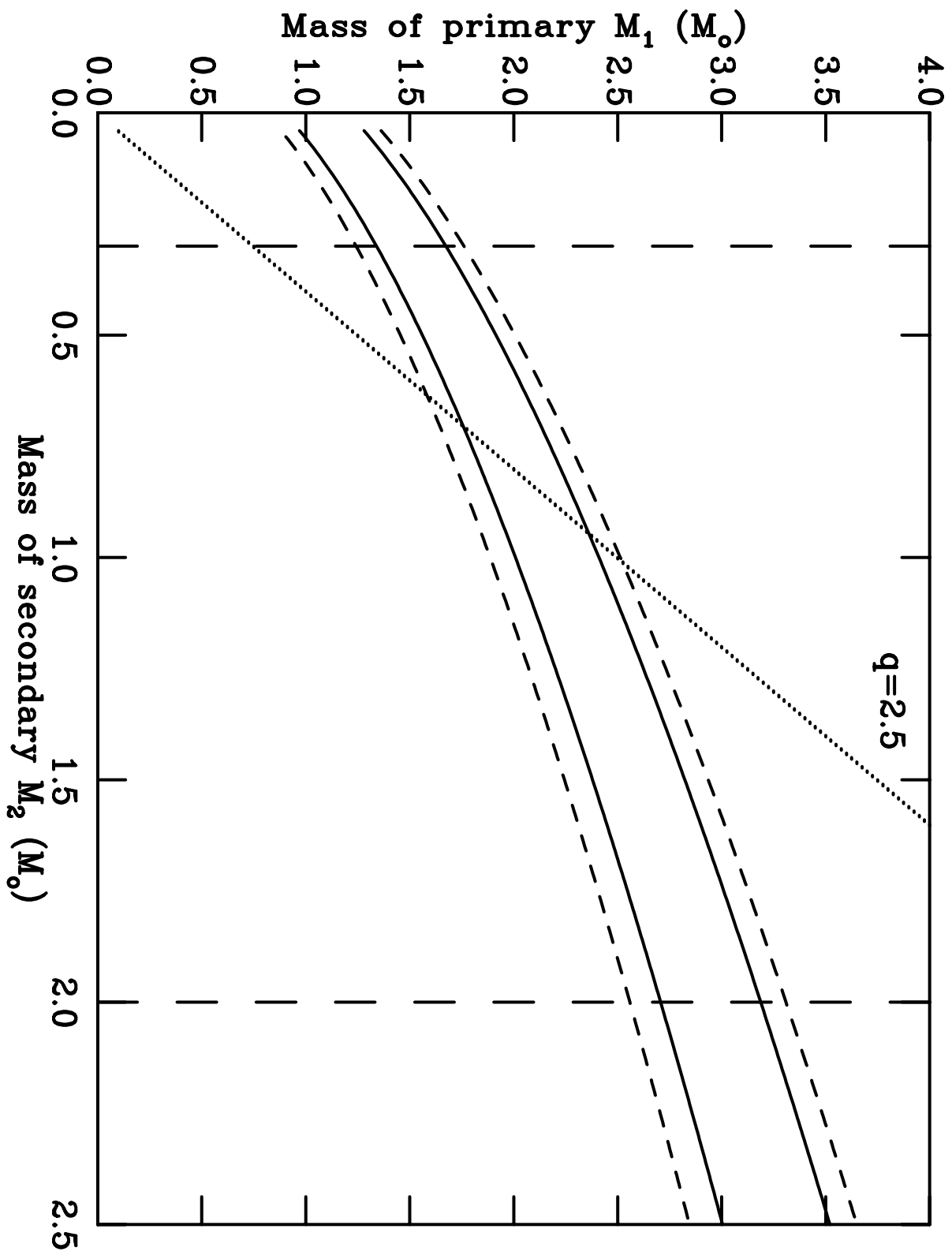


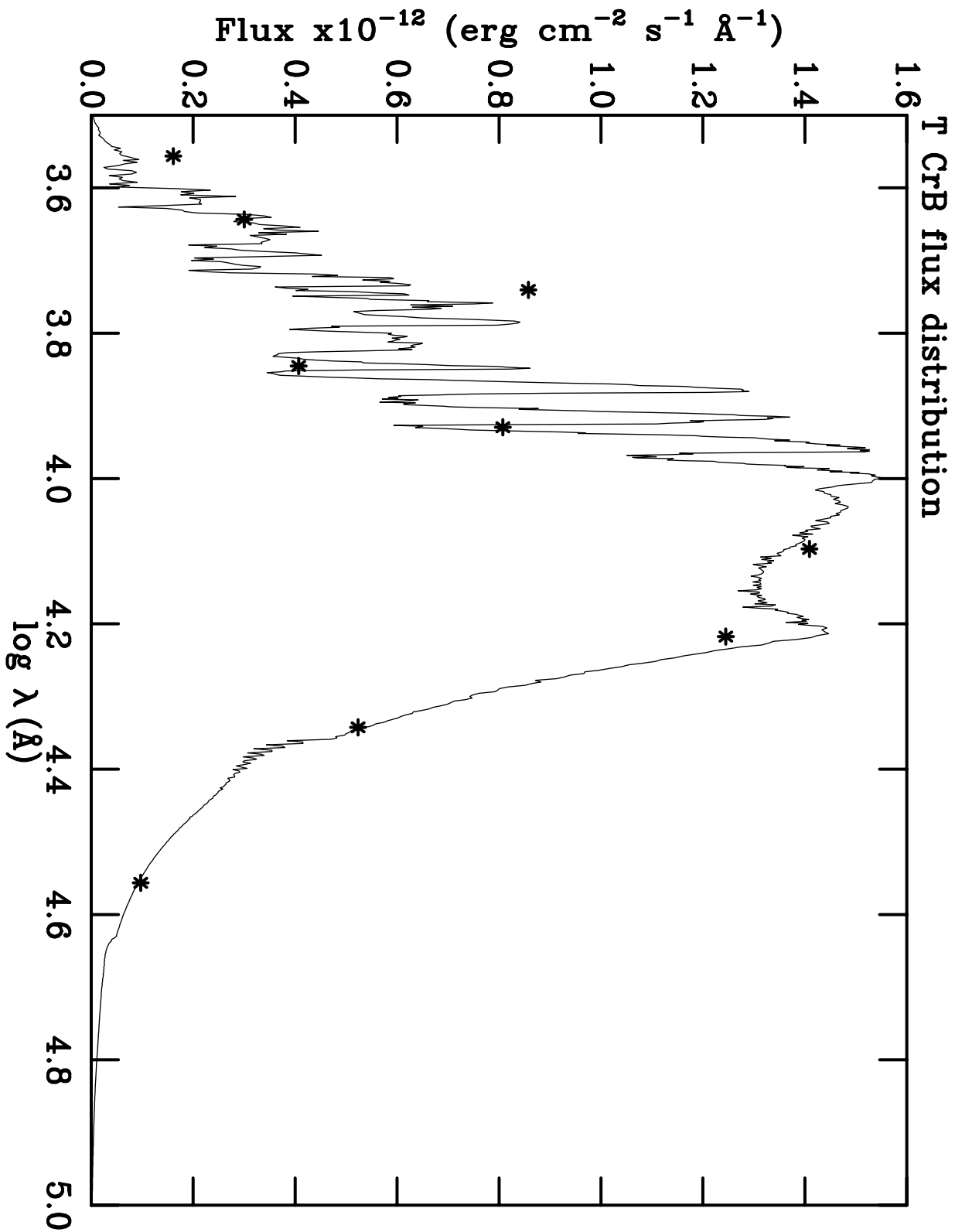












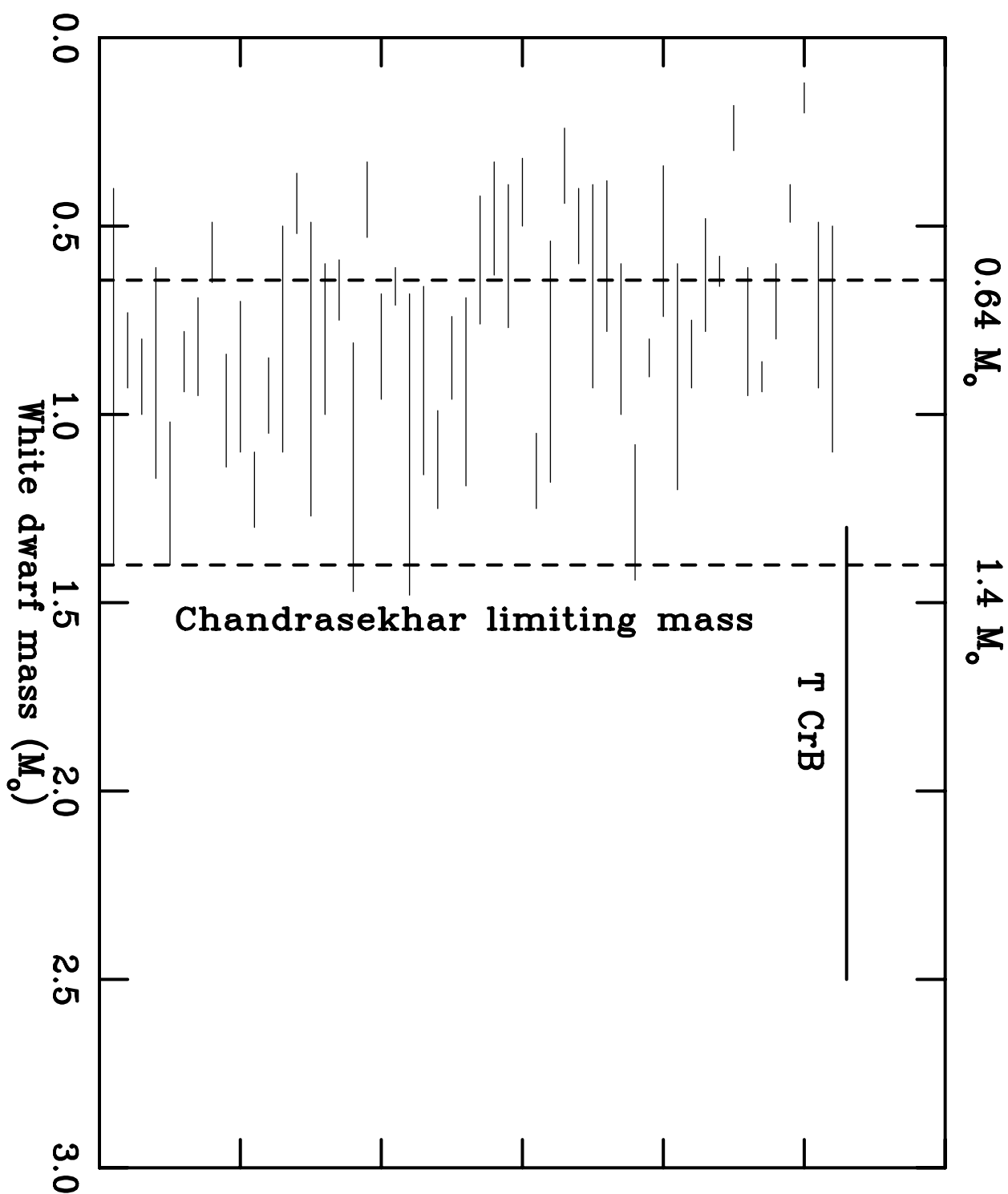


Figure captions.

Figure 1. The individual I , J , H and K band light curves of T CrB folded on the orbital ephemeris given by Kenyon & Garcia (1986). The data are plotted over 1.5 cycles.

Figure 2. The J band light curve with model fits. The dotted line is a fit using $q=3$, $\beta=0.08$, $i=48^\circ$ and the solid line is a fit using $q=3$, $\beta=0.20$ and $i=43^\circ$. Note that these two fits are very similar. The dashed line is a fit using $q=3$, $\beta=0.08$, $i=43^\circ$ and $R_{\text{spot}}=20^\circ$. As one can see, the best fit to the light curve is the one with the dark spot (see text).

Figure 3. The 68 percent confidence level solutions for model fits to the J band data in the $\beta - i$ plane, obtained by collapsing the minimum χ^2 solutions along the q axis. The cross marks the best solution.

Figure 4. The 68 percent confidence level solutions for model fits to the J band data using $\beta=0.08$. The solutions in the $R_{\text{spot}} - i$ plane were obtained by collapsing the solutions along the q axis onto the $R_{\text{spot}} - i$ plane. The cross marks the best solution.

Figure 5. The temperature distribution of the secondary star along the line joining the centre of mass of the binary components (x/a ; where x is the distance and a is the binary separation). The solid lines show the distribution using $\beta=0.08$ and 0.20 , and the dotted lines show the distribution using $\beta=0.08$ plus a dark spot of radius 20° .

Figure 6. The allowed mass range for the compact object obtained by combining the inclination limits derived from the J band data with the mass function. The solid and dashed lines are the 68 and 90 per cent confidence limits respectively. We also show the lower limit to the mass ratio $q=2.5$ (dotted line) obtained by Kenyon & Garcia (1986) and the bounds to the mass of the secondary star (long dashed lines; see section 6). We limit the compact object to lie in the mass range $1.3\text{--}2.5 M_\odot$ (90 percent confidence).

Figure 7. The optical and infrared magnitudes of T CrB, taken from Munari et al. (1992) and dereddened using $E_{B-V}=0.15$ (Selvelli, Cassatella & Gilmozzi 1992). The thin weighted line shows a fit with a M3 III model atmosphere flux distribution (Kurucz 1992).

Figure 8. The mass distribution of white dwarfs. The data were taken from Ritter & Kolb (1995). The dashed lines at $0.64 M_\odot$ and $1.4 M_\odot$ mark the observed white dwarf mass (weighted average) and the Chandrasekhar limiting mass respectively. Also shown is the mass of the white dwarf in T CrB (90 per cent confidence).